

NATIONAL RADIO ASTRONOMY OBSERVATORY
GREEN BANK, WEST VIRGINIA

ELECTRONICS DIVISION INTERNAL REPORT No. 165

ATMOSPHERIC CONTRIBUTION TO SYSTEM NOISE

J. RICHARD FISHER

MAY 1976

NUMBER OF COPIES: 150

ATMOSPHERIC CONTRIBUTION TO SYSTEM NOISE

J. Richard Fisher

Introduction

Here is a summary of atmospheric radiation between 1 and 100 GHz from the literature and a few 140-foot measurements below 15 GHz. Most of it is sort of "common knowledge" but I have not seen it all put together in a boiled down form before. This is by no means a complete literature search and is only intended as a rough outline with applications to the new low noise maser systems in mind. A much more detailed discussion of the theory of uncondensed gases is given by LeFande (1973).

Absorption in this frequency range is usually broken down into five constituents: non-resonant O₂, resonant O₂ (~ 0.5 cm), resonant water vapor (1.34 cm), residual water vapor (composite line wings), and condensed water. Below 15 GHz the main contributors are non-resonant O₂ which is nearly independent of frequency and condensed water which is very frequency, bulk volume and drop size dependent, its absorption rising rapidly between 10 and 1 cm. A rather nice plot of the relative contributions of the vapor constituents is given by LeFande (1973) (Figure 1), although the magnitude of the O₂ non-resonant part is too high.

Non-Resonant O₂ Absorption

This component is due to the excitation of the permanent magnetic moment of the oxygen molecule and losses due to collisions. This is a very weak interaction but amounts to about 0.03 dB over the vertical ground to space path (0.1 dB \approx 7 K added noise). The non-resonant O₂ absorption at 300 MHz is only about one third of that at 1 GHz, but between 1.4 GHz and 15 GHz this absorption rises less than 20% or so. The form of the frequency dependence of the

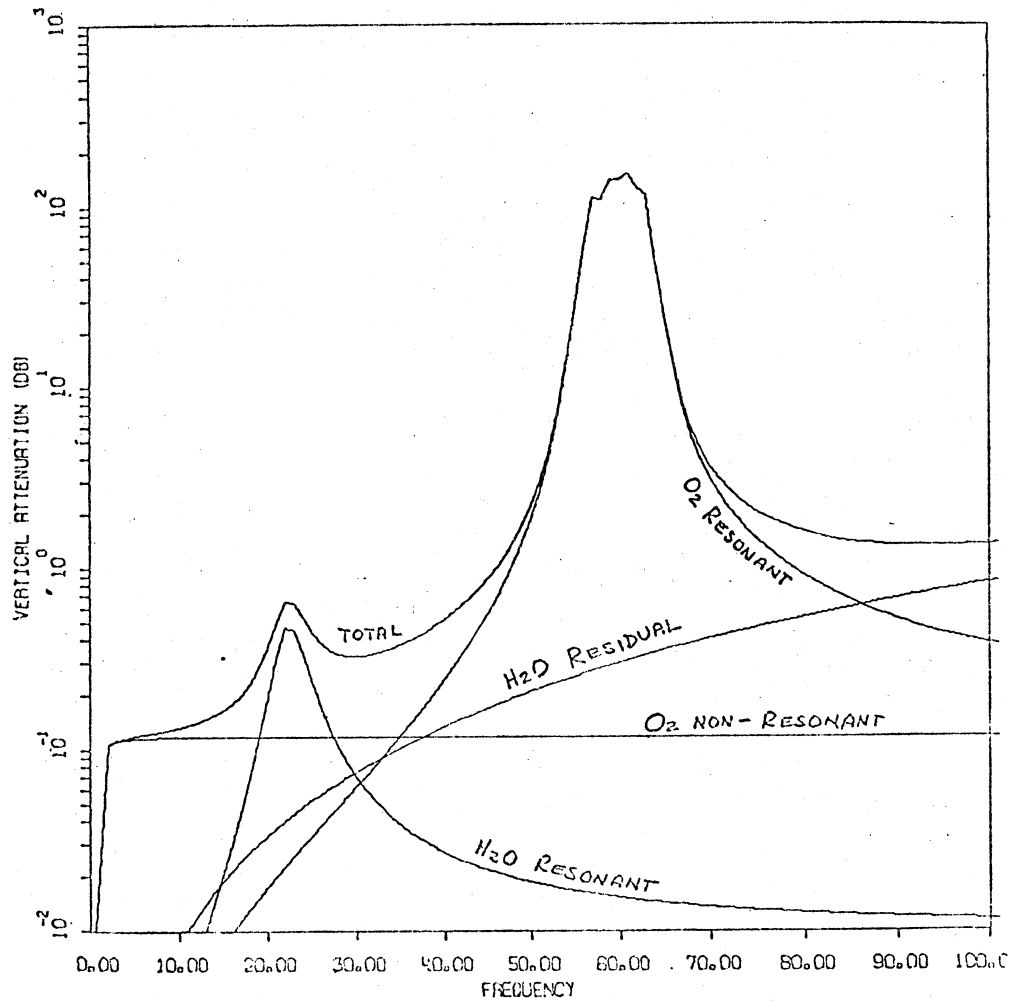


FIGURE 1

Attenuation for a vertical path with contributing terms plotted vs. frequency computed from the model atmosphere with semi-empirical expressions for the absorption coefficients and $AH_0 = 7.0 \text{ g/m}^3$.

absorption coefficient is

$$\gamma \propto \frac{\nu^2}{\nu^2 + \Delta\nu^2}$$

(cf. Kerr, 1951) where $\Delta\nu$ is a line breadth constant on the order of 1 GHz/atmosphere (LeFande, 1973) for O_2 . The distinction between resonant and non-resonant absorption is a bit artificial as can be seen from the fact that a line breadth constant crops up in the non-resonant equation. For $\nu \gg \Delta\nu$, γ is

a constant. Note when reading LeFande's thesis, the non-resonant O₂ absorption calculated is high by a factor of 4 or so for some reason.

Resonant O₂ Absorption

Above 15 GHz the resonant terms of O₂ and H₂O become important. The first microwave resonance of molecular O₂ is at 60 GHz, and the absorption in the center of this line is about 100 dB at the zenith as seen in Figure 1. This component is of little importance below 30 GHz, but it dominates the absorption between about 40 and 80 GHz.

Resonant Water Vapor Absorption

The lowest frequency resonant atmospheric absorption comes from uncondensed water vapor at 22 GHz. Because of the relatively small scale height and variable water content in the atmosphere the absorption near this line is quite dependent on the distribution of H₂O with height and the altitude of the observing site. Even if the total water content in the atmosphere remains constant, the absorption in the wings depends on collisional broadening; more water at high altitudes makes a narrower line.

Figure 2 shows a few radiosonde samples of the water vapor distribution over Massachusetts in the summer (Staelin, 1966). Note that the total water content is poorly correlated with the density at the surface.

The shaded area in Figure 3 shows the range of atmospheric noise contributions at the zenith in the 20-30 GHz range measured over the same period as the water contents in Figure 2. There seems to be a loose correlation of total water vapor with atmospheric noise in this frequency range, but the experimental problems make this correlation difficult to establish. Also shown in Figure 3 are ranges of three frequency measurements made by Dicke, et al. (1946) in

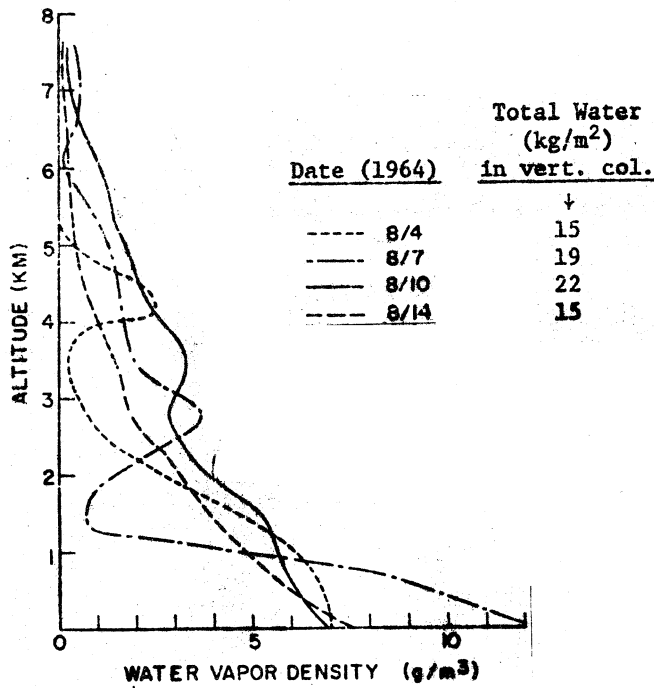


FIGURE 2

Distribution of water vapor density over Massachusetts for four of the days on which noise measurements in Figure 3 were made.

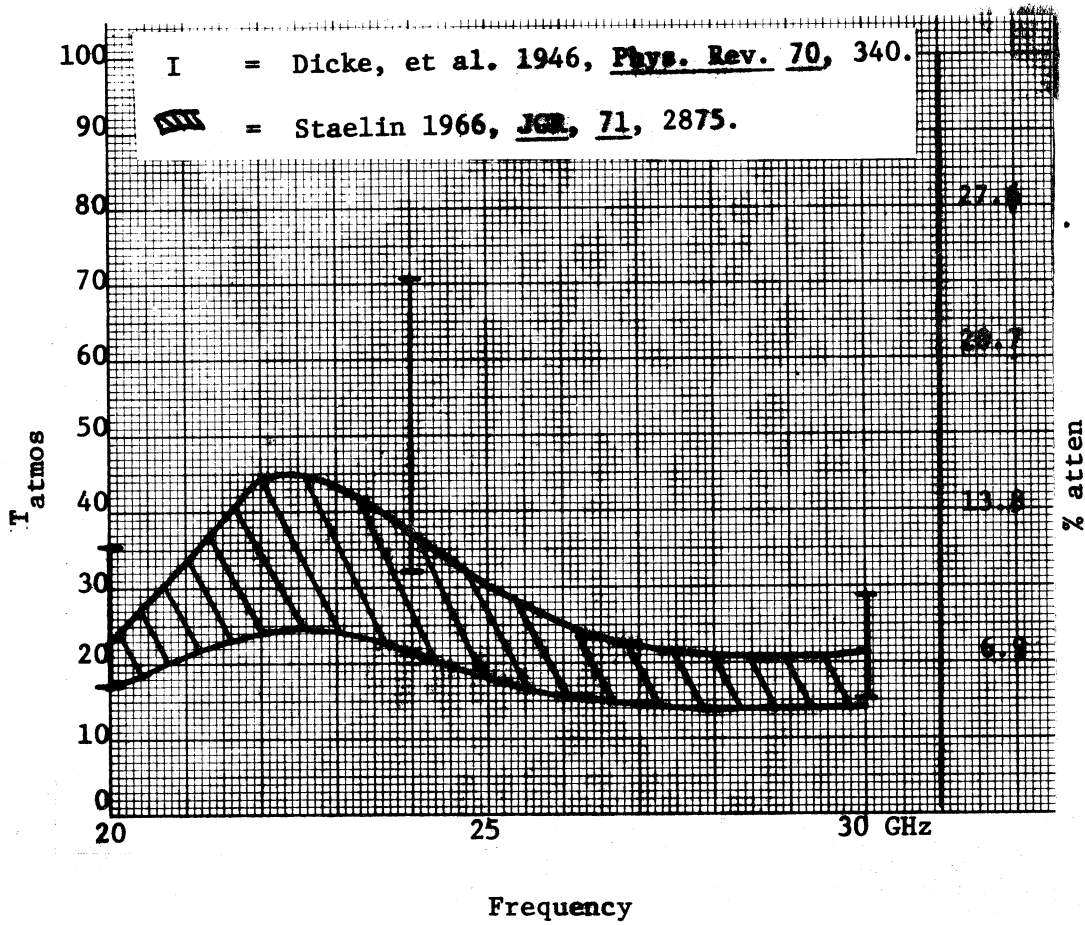


FIGURE 3

Atmospheric noise measured between 20 and 30 GHz under rather humid conditions.

Florida. Total water vapor ranged from 20 to 38 kg/m² in this case. Both of these sets of measurements were made under rather humid conditions. Total water vapor contents on clear winter days over Green Bank can be less by more than a factor of ten so it would seem reasonable to expect comparable reductions in atmospheric noise, occasionally, around 22 GHz.

Residual Water Vapor Absorption

The density of water vapor lines increases considerably above 100 GHz. However, the combined effect of the absorption in the collisionally broadened wings of these lines is quite substantial as low as 20 GHz. This composite absorption is called residual H₂O absorption and is proportional to $1/\lambda^2$ in the centimeter and millimeter microwave range. The $1/\lambda^2$ dependence is one of the main reasons for the higher and higher absorption in the shorter wavelength windows. As one might expect the bulk of atmospheric absorption due to this component occurs at low altitudes where pressure (collisional) broadening of the high frequency lines is the greatest. Hence, it is very dependent on the detailed height distribution of water vapor over the observing site.

Condensed Water Absorption

Water droplets in the atmosphere cause microwave path loss by both absorption and scattering. For drops which are small compared to a wavelength the absorption is predominant; hence, the loss also adds noise like any resistive attenuator. The mechanism is simply heating from induced currents in a lossy dielectric. For very fine water particles as in fog or clouds the attenuation below 100 GHz at 18°C is accurately described by

$$\gamma = 0.44 M/\lambda^2 \quad (\text{dB/km})$$

(Kerr, 1951) or for small attenuations the added noise is

$$T = 29 M/\lambda^2 \quad (\text{Kelvins/km})$$

where M is the mass density of water in g/m² and λ is in centimeters. Table 1 from Kerr (1951) gives the absorption correction factors in this case for various wavelengths and water temperatures. Typical fog and cloud densities are given in the caption of Figure 4 (Kerr, 1951).

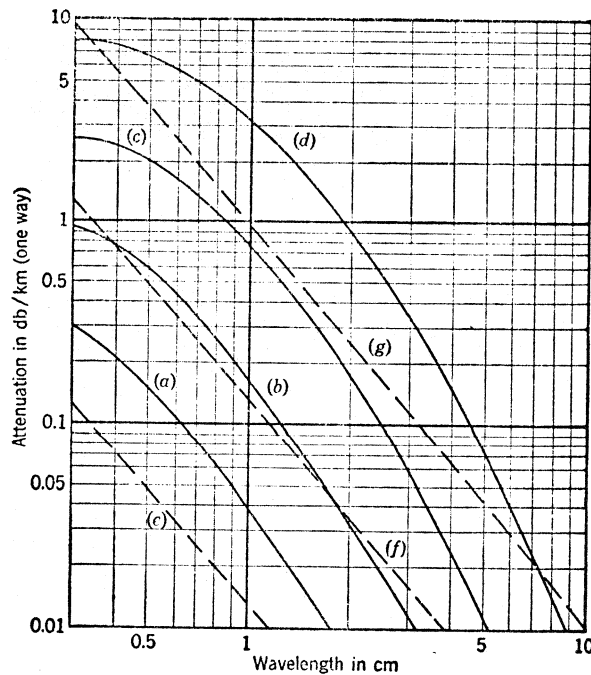
$$c_1(T) = \phi_1(T) c_1(18^\circ).$$

TABLE 1
Correction Factor $\phi_1(T)$ for Coefficient c_1 *

λ, cm	0°C	10°C	18°C	20°C	30°C	40°C
0.5	1.59	1.20	1.0	0.95	0.73	0.59
1.25	1.93	1.29	1.0	0.95	0.73	0.57
3.2	1.98	1.30	1.0	0.95	0.70	0.56
10.0	2.0	1.25	1.0	0.95	0.67	0.59

* After Ryde and Ryde.

For larger drop sizes (rain) or shorter wavelengths the $1/\lambda^2$ dependence of the absorption no longer holds. The absorption increases less rapidly with decreasing wavelength for larger drops so a detailed knowledge of the drop size distribution is necessary to calculate absorption in rain. From arguments concerning drop terminal velocities mixed with a bit of empirical information, estimates of the drop size distribution have been made for different rain rates, and the associated absorption as a function of wavelength has been computed. The results are shown in Figure 4 (Kerr, 1951) along with the absorption in fog. Briefly, the absorption and associated noise due to rain or fog is negligible longward of 10 cm. At 3 cm light rain or moderately dense fog can contribute



Theoretical values of attenuation by rain and fog. Solid curves show attenuation in rain of intensity. (a), 0.25 mm/hr (drizzle); (b), 1 mm/hr (light rain); (c), 4 mm/hr (moderate rain); (d), 16 mm/hr (heavy rain). Dashed curves show attenuation in fog or cloud. (e), 0.032 g/m³ (visibility about 2000 ft); (f), 0.32 g/m³ (visibility about 400 ft); (g), 2.3 g/m³ (visibility about 100 ft).

FIGURE 4

about one Kelvin to the system temperature with moderate rain or severe fog adding 15 K or so, all of this assuming a path length of one kilometer. At 1 cm a light rain or moderate fog adds about 10 K with heavy rains making observations impossible.

Estimates of attenuation due to dry snow or hail are much more difficult, but in any case it is much smaller than for comparable rain precipitation rates. Very wet snow can be rather absorptive, however,

Another manifestation of condensed water absorption is the attenuation by a bulk water layer such as observing through a wet radome. Figures 5 and 6 (Hogg, 1975) show the effects of layered water absorption between 1 and 3 cm. It appears that a layer of water only 1 micrometer thick on a radome will add

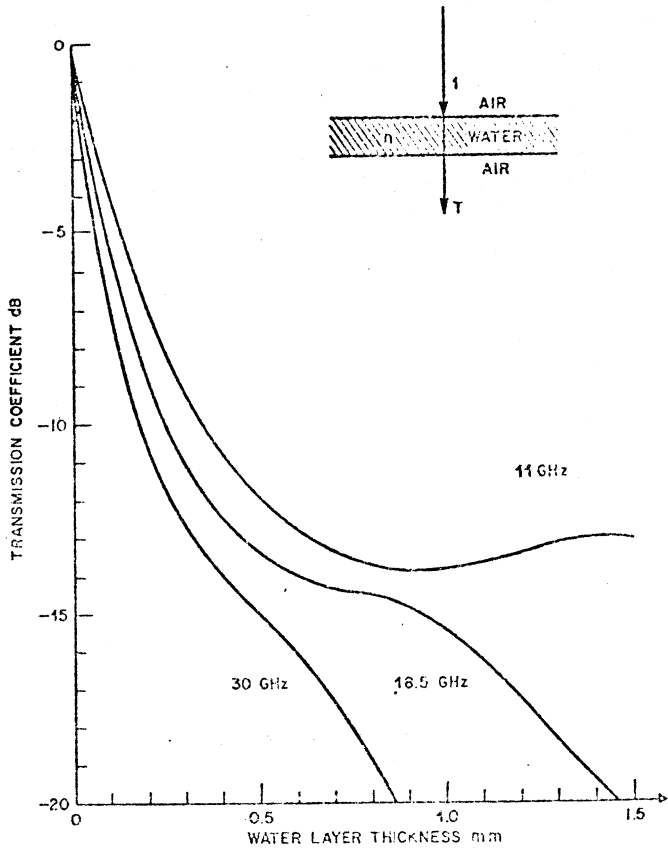


FIGURE 5

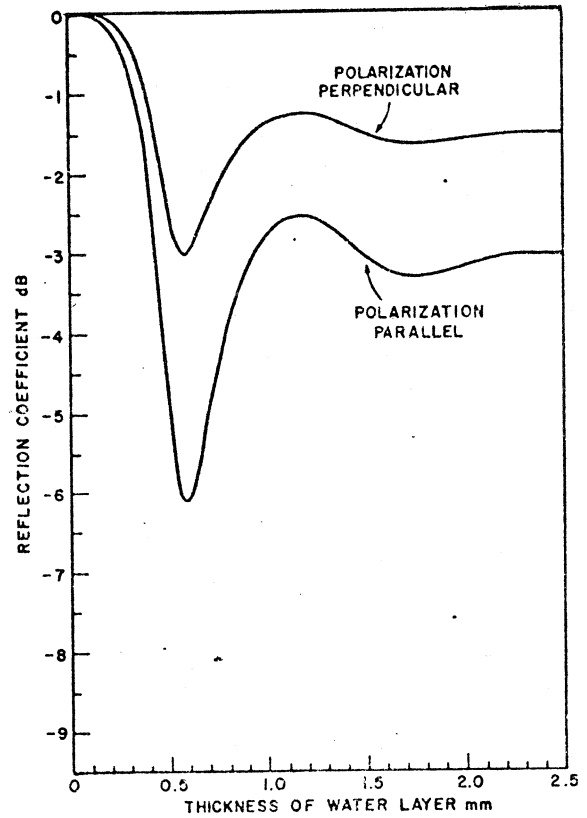


FIGURE 7

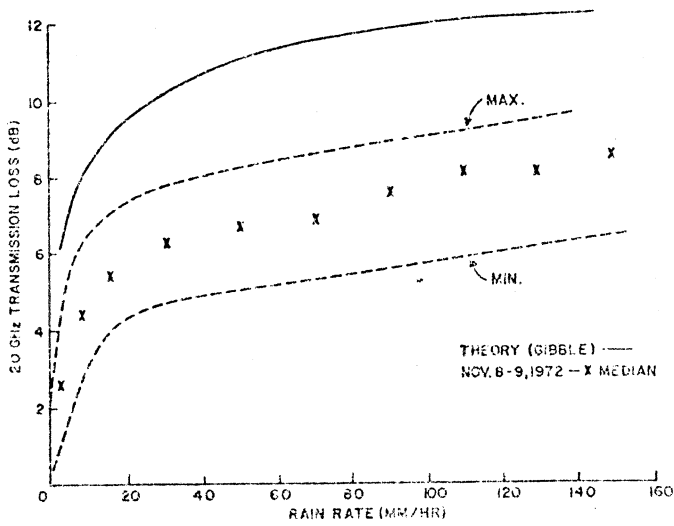


FIGURE 6

about 10 K to the antenna temperature through a radome at 30 GHz. On the other hand, water on a reflecting surface such as an exposed dish has a negligible effect as can be seen in Figure 7 from Hogg (1975). A thick layer of wet snow is another matter, however. Even at 1.4 GHz a couple of inches of melting snow has been seen to cause an increase in system temperature of about 30 K on the 300-foot. The same snow just a few degrees colder had a negligible effect on the system temperature.

Sky Noise Measurements Between 1.4 and 15 GHz

System temperature versus zenith distance measurements were made in March and April 1976 at 1.4, 10.8, and 14.7 GHz on the 140-foot prime focus systems. The results are shown in Figures 8(a) through (g). Clear or nearly clear weather existed for at least one of the measurements at each frequency (Figures 8a, c, d, f, and g). The slope of the T vs $(1 - \sec z)$ line fit by eye gives the average atmospheric radiation at the zenith. On clear days the scatter around this straight line is quite small so the zenith excess noise is well determined. The uncertainties in the radiometers' internal noise references are about $\pm 3\%$ at 1.4 GHz, $\pm 10\%$ at 10.8 GHz and $\pm 20\%$ at 14.7 GHz.

The actual atmospheric radiation along the beam line-of-sight is about 20% higher than measured because some of the antenna's radiation pattern is spread isotropically around the sky, and the radiation received in the far sidelobes is, on the average, not dependent on antenna position. Also, the curvature of the earth causes a deviation from the $\sec z$ dependence below about 6° elevation. There is an added complication that if there is much ground radiation in the feed spillover pattern there will be a distortion of the high elevation part of the curve. However, this problem should be insignificant in the 8° to 30° elevation range where the $(1 - \sec z)$ coefficient is best determined.

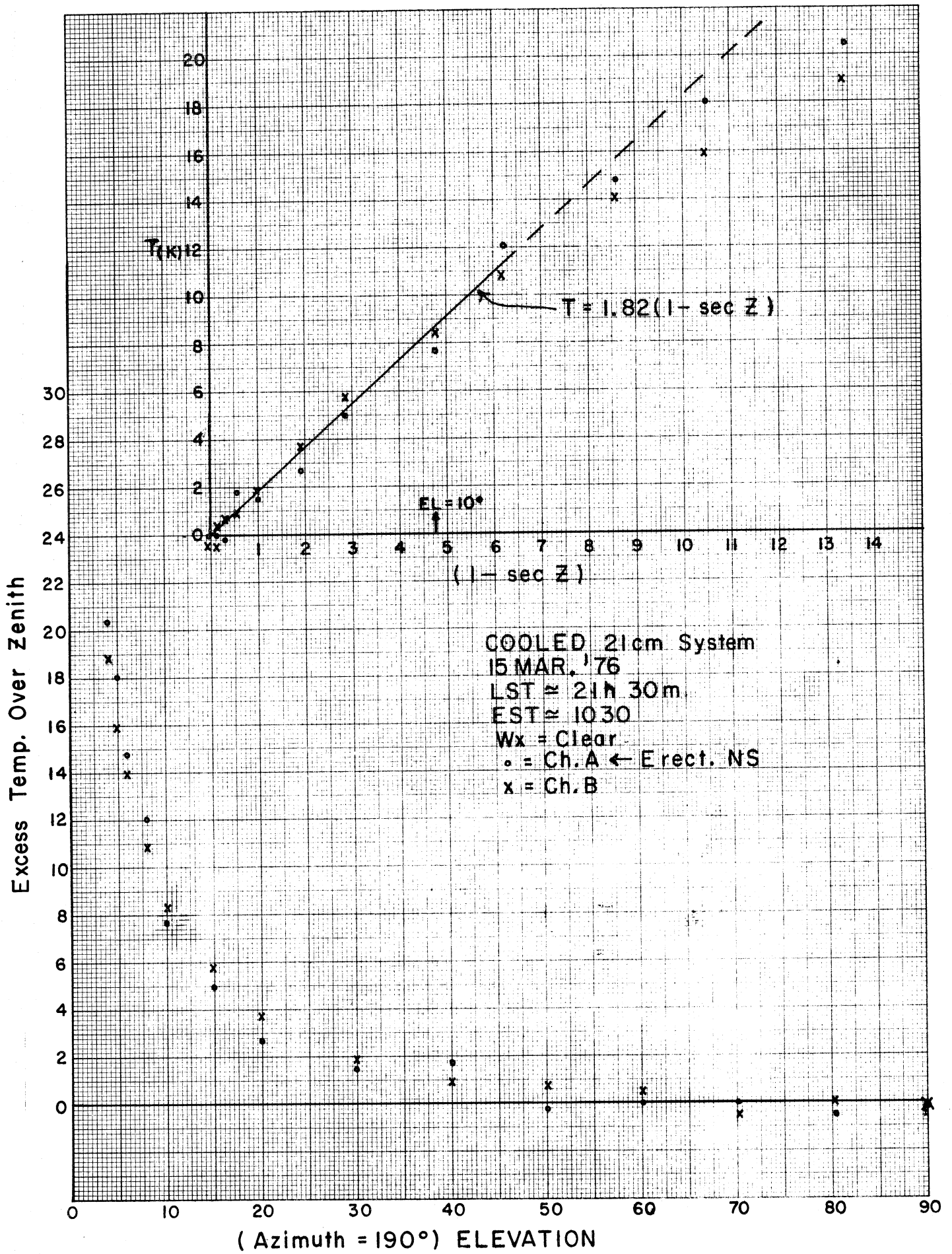
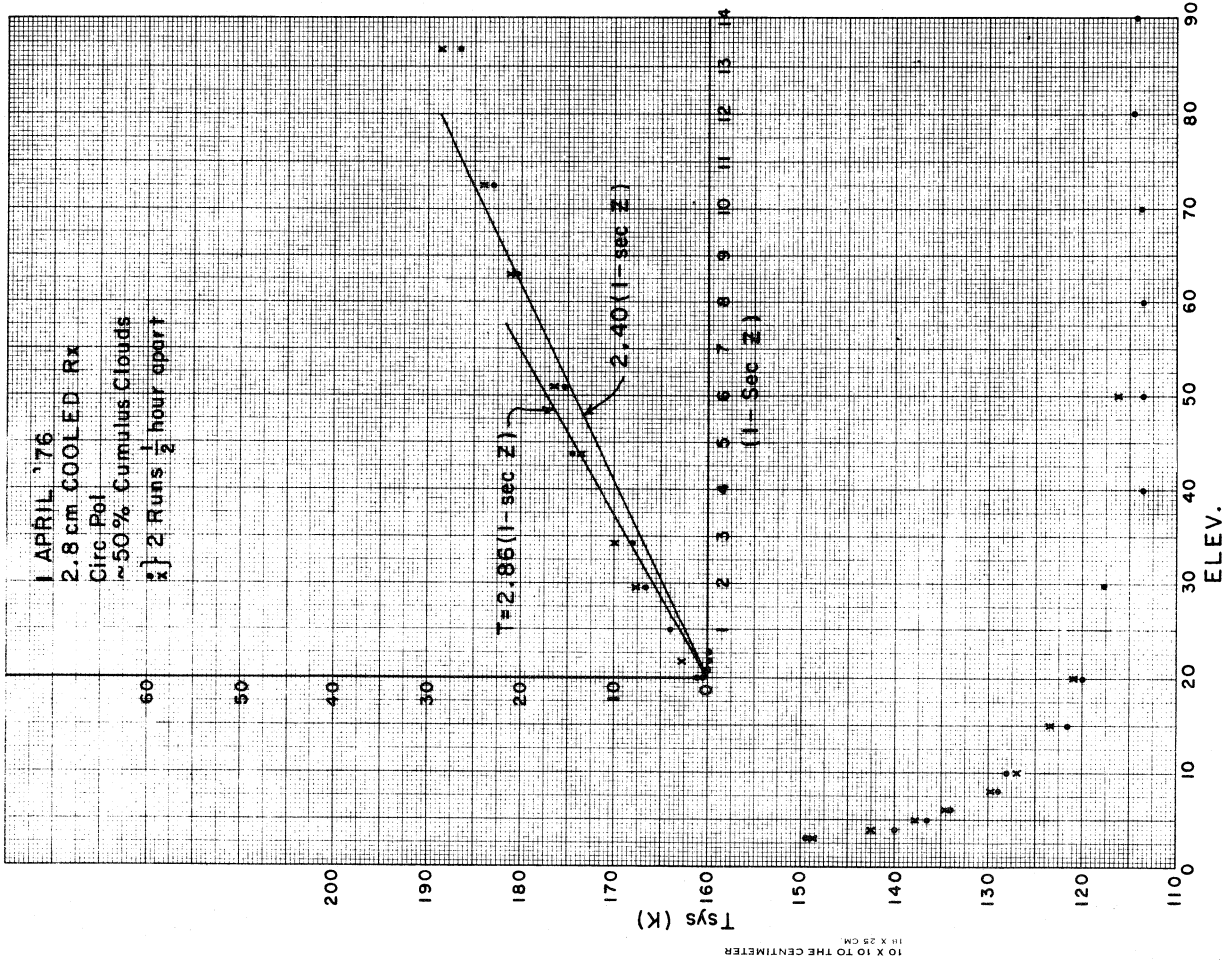
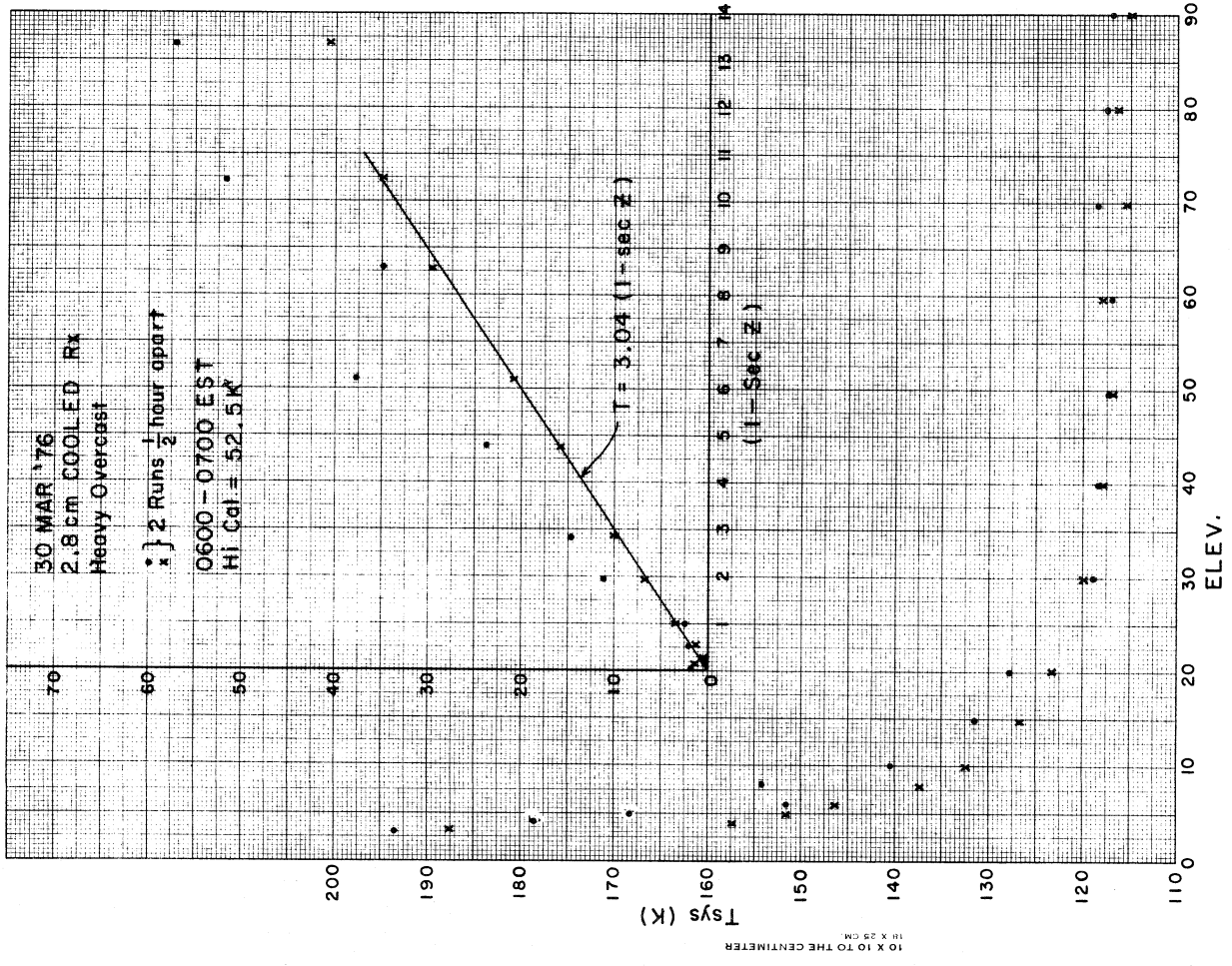


FIG. 8 (a)



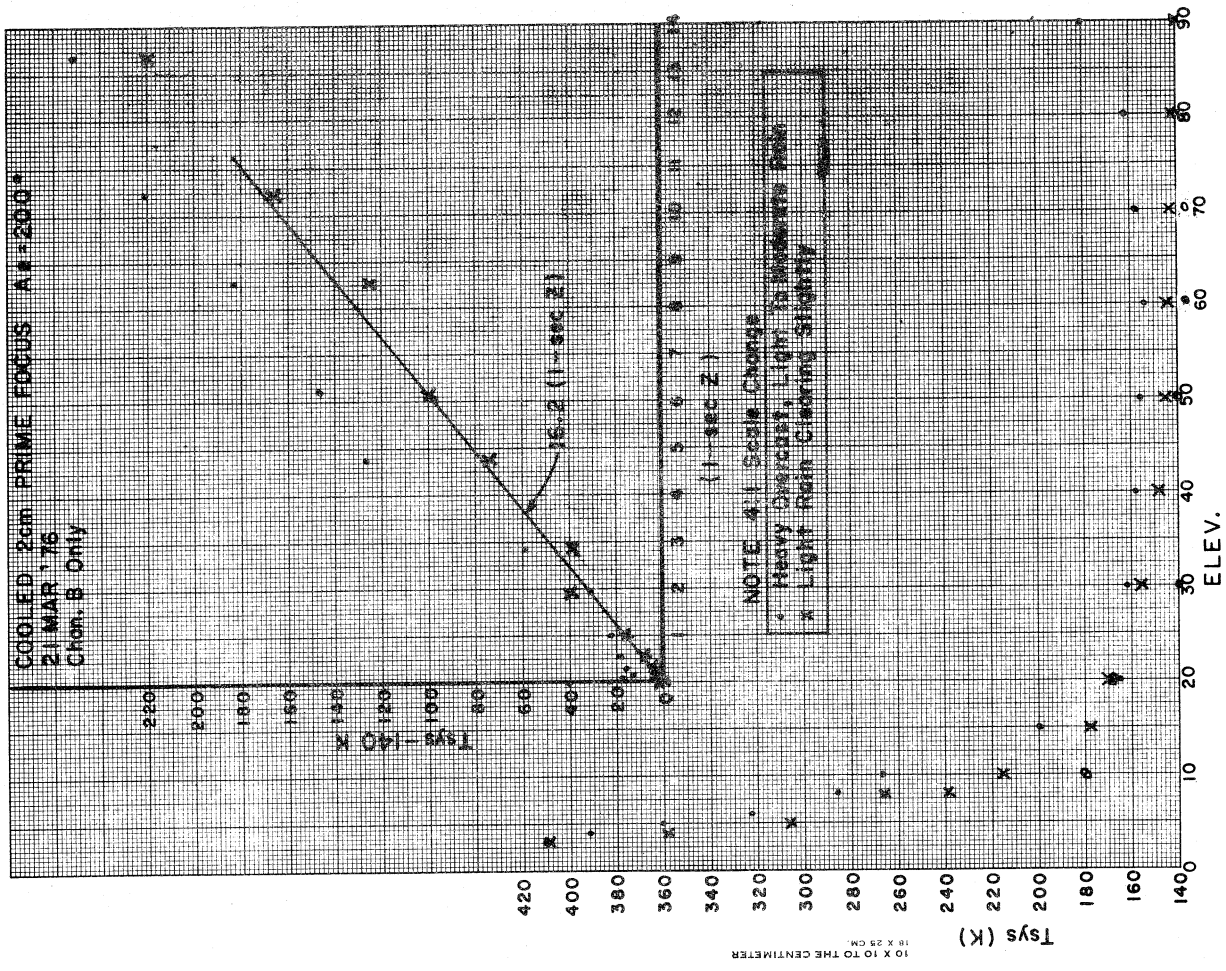


FIG. 8(e)

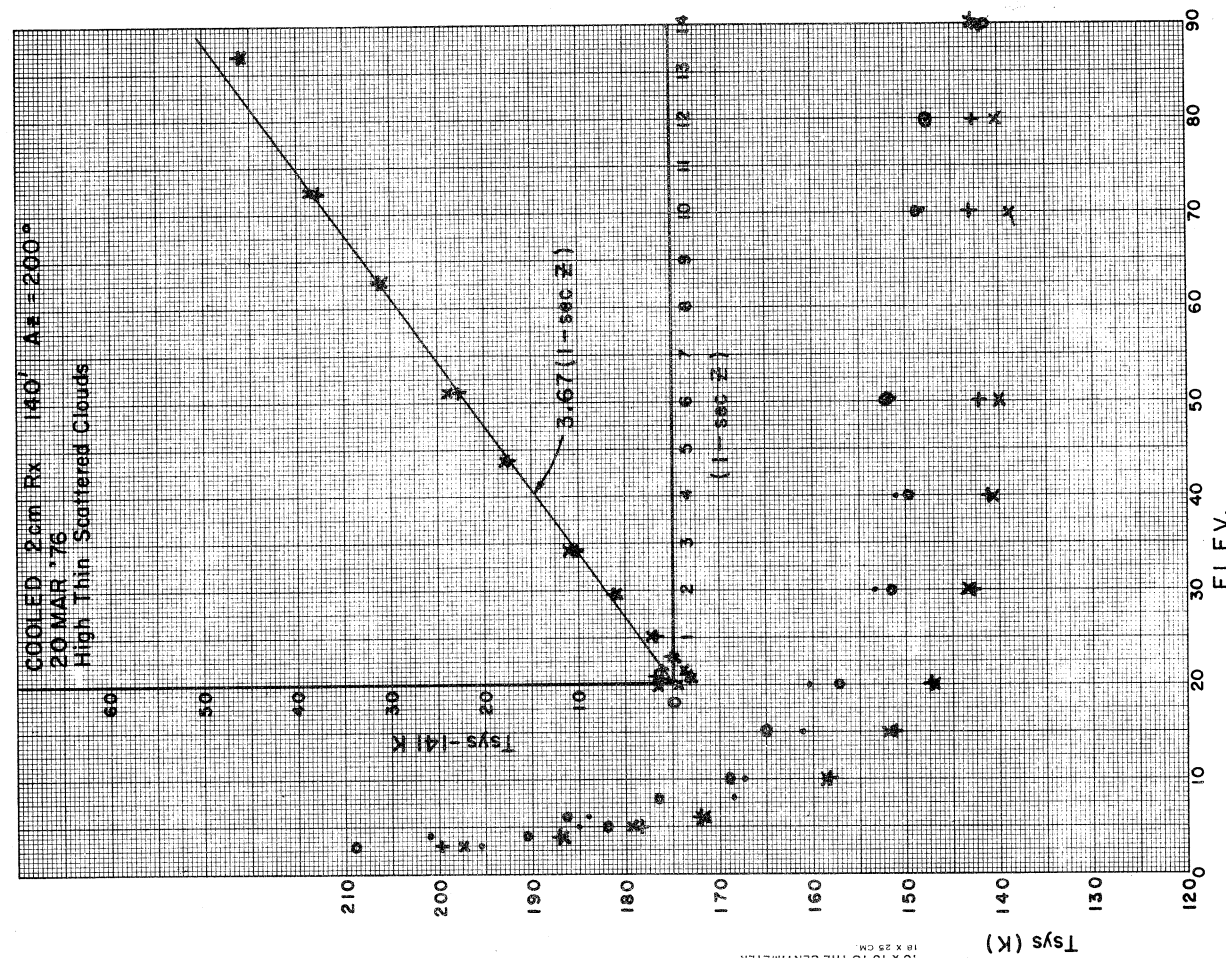
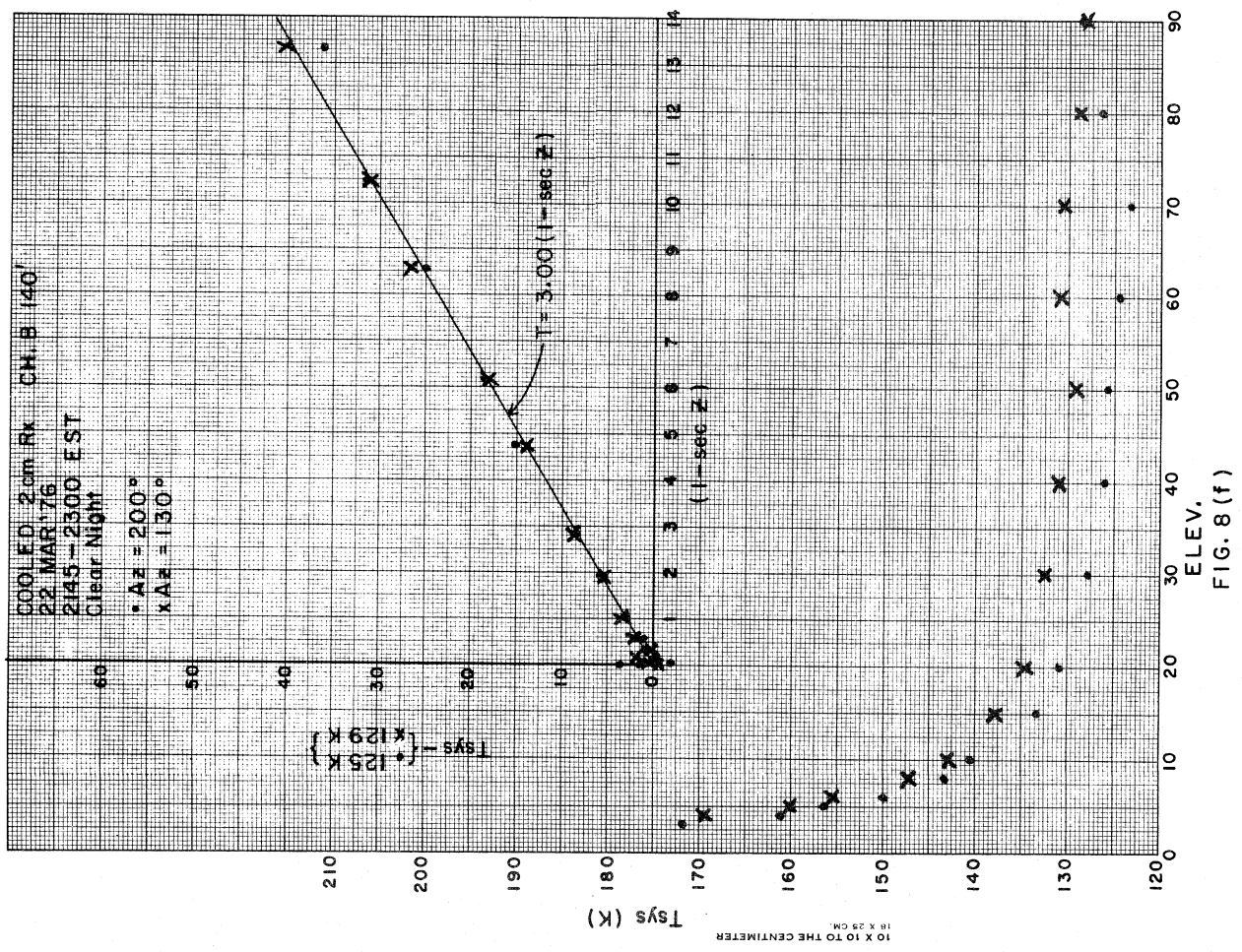
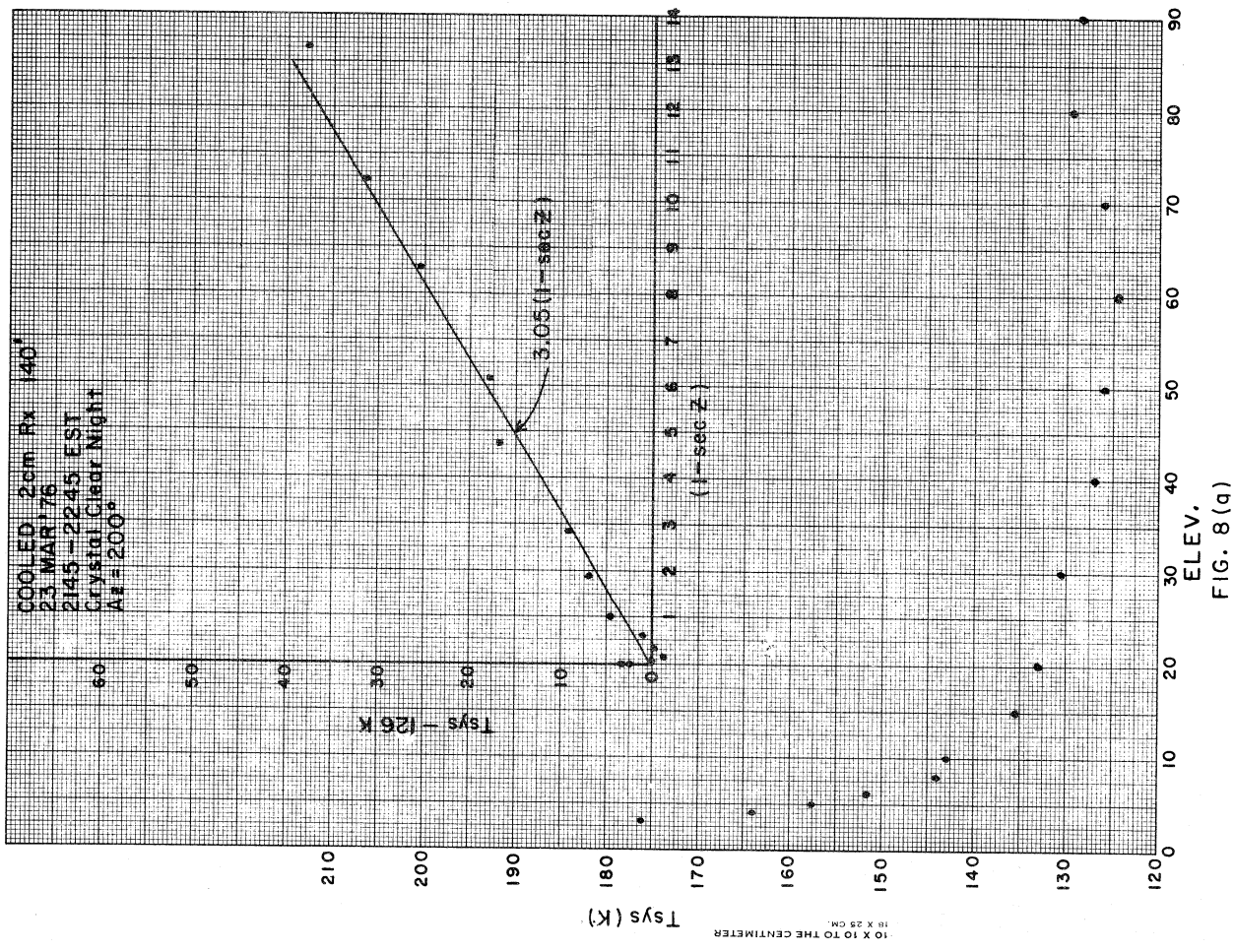


FIG. 8(d)



Additional measurements are published for the Goldstone 64-meter antenna (Reid, et al., 1973) and are shown in Figure 9. Estimated coefficients from this graph are 2.3 K at 2.2 GHz, 3.0 K at 8.4 GHz, and 3.2 K at 15.3 GHz under desert conditions.

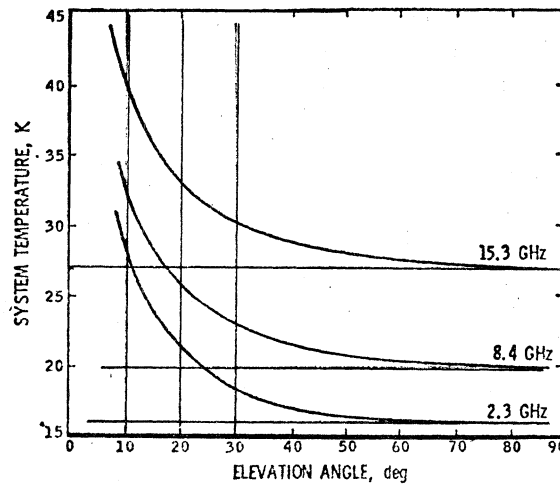


FIGURE 9

System operating noise temperature as a function of antenna elevation angle on the Goldstone 210-foot.

Summary

Figure 10 is an estimate based mainly on experiment of the atmospheric contribution to system temperature between 1 and 30 GHz that can be expected in Green Bank on clear days. Below 3 GHz the only loss is from non-resonant molecular oxygen. Water vapor, clouds, or moderate rain have virtually no effect.

Between 3 and 15 GHz residual water vapor absorption and clouds and rain become increasingly important. One example of a 5-fold increase in absorption due to rain and dense clouds at 14.7 GHz is shown in Figure 8(e). However,

some clouds have a relatively small effect at least at 10.8 GHz (Figure 8(b)). This is more or less consistent with the absorption predicted in Figure 4.

Above about 17 GHz water vapor resonant absorption is dominant on clear days. The effects of rain and clouds are also higher in this frequency range sometimes making observations very difficult.

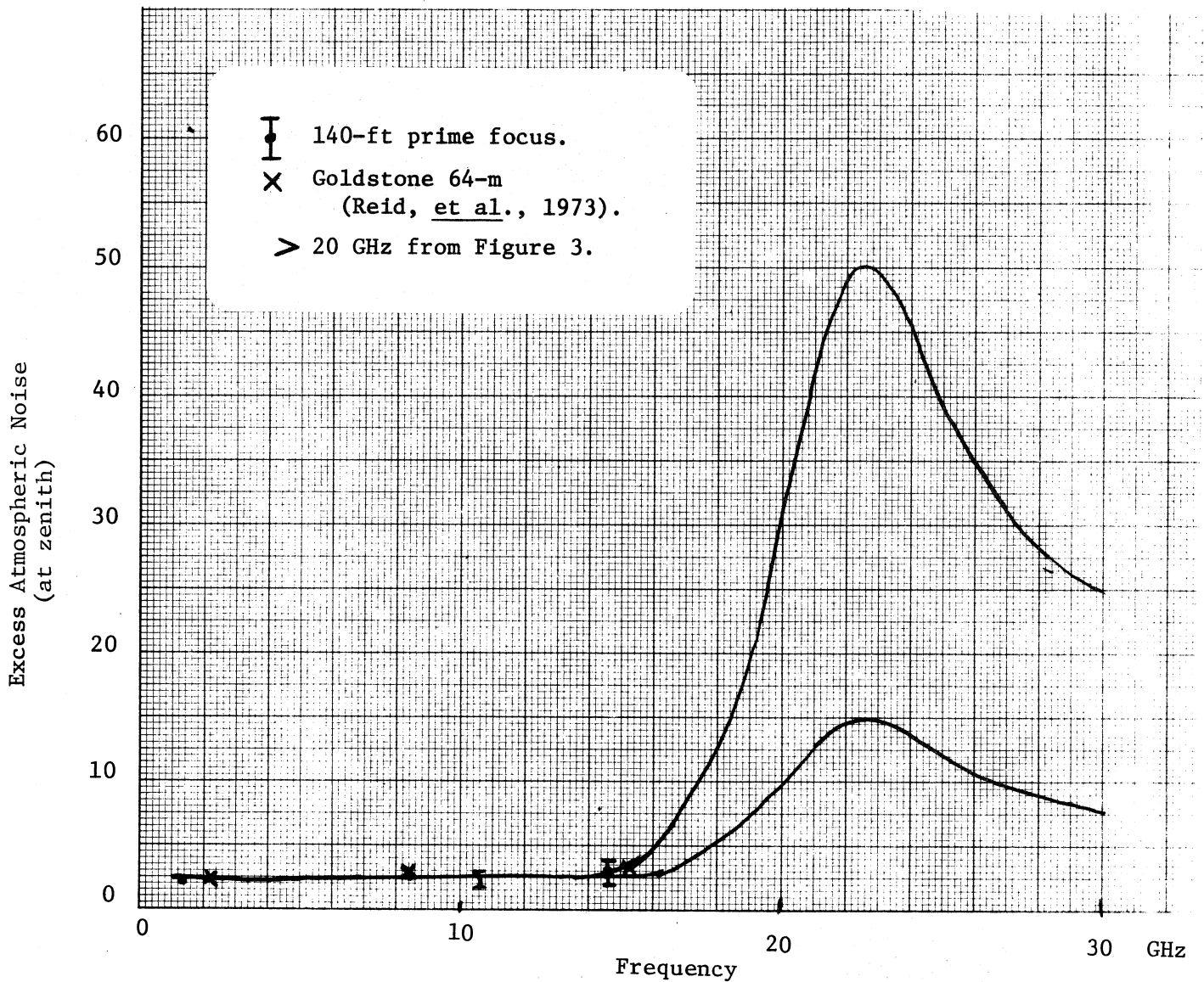


FIG. 10

REFERENCES

Kerr, D. E. 1951, M.I.T. Radiation Laboratory Series 13. 650 (ch. by J. H. VanVleck).

LeFande, R. A. 1973, U. of Md., Ph.D. thesis.

Staelin, D. H. 1966, J.G.R., 71, 2875.

Dicke, R. H., Beringer, R., Kyhl, R. L. and Vane, A. B., Phys. Rev. 70, 340.

Hogg, D. C. 1975, Proc. IEEE, 63, 1308.

Reid, M. S., Clauss, R. C., Bathker, D. A. and Stelzried, C. T. 1973, Proc. IEEE, 61, 1330.